Biochimica et Biophysica Acta 1830 (2013) 3517–3524

Contents lists available at SciVerse ScienceDirect

Biochimica et Biophysica Acta

journal homepage: www.elsevier.com/locate/bbagen

Non-invasive label-free monitoring the cardiac differentiation of human embryonic stem cells in-vitro by Raman spectroscopy

Flavius C. Pascut [a], Spandan Kalra [b], Vinoj George [b], Nathan Welch [a], Chris Denning [b], Ioan Notingher [a,*]

[a] School of Physics and Astronomy, University of Nottingham, University Park, Nottingham, NG7 2RD, UK
[b] Wolfson Centre for Stem Cells, Tissue Engineering & Modelling, Centre for Biomolecular Sciences, University Park, University of Nottingham, Nottingham, NG7 2RD, UK

ARTICLE INFO

Article history:
Received 18 September 2012
Received in revised form 28 January 2013
Accepted 30 January 2013
Available online 9 February 2013

Keywords:
Embryoid body
Human embryonic stem cell
Differentiation
Cardiomyocyte
Raman spectroscopy

ABSTRACT

Background: Online label-free monitoring of in-vitro differentiation of stem cells remains a major challenge in stem cell research. In this paper we report the use of Raman micro-spectroscopy (RMS) to measure time- and spatially-resolved molecular changes in intact embryoid bodies (EBs) during in-vitro cardiogenic differentiation.
Methods: EBs formed by aggregation of human embryonic stem cells (hESCs) were cultured in defined medium to induce differentiation towards cardiac phenotype and maintained in purpose-built micro-bioreactors on the Raman microscope for 5 days (between days 5 and 9 of differentiation) and spatially-resolved spectra were recorded at 24 h intervals.
Results: The Raman spectra showed that the onset of spontaneous beating of EBs at day 7 coincided with an increase in the intensity of the Raman bands at 1340 cm^{-1}, 1083 cm^{-1}, 937 cm^{-1}, 858 cm^{-1}, 577 cm^{-1} and 482 cm^{-1}. The spectral maps corresponding to these bands had a high positive correlation with the expression of the cardiac-specific α-actinin obtained by immuno-fluorescence imaging of the same EBs. The spectral markers obtained here are also in agreement with previous studies performed on individual live hESC-derived CMs.
Conclusions: The intensity profile of these Raman bands can be used for label-free in-situ monitoring of EBs to estimate the efficacy of cardiogenic differentiation.
General significance: As the acquisition of the time-course Raman spectra did not affect the viability or the differentiation potential of the hESCs, this study demonstrates the feasibility of using RMS for on-line non-invasive continuous monitoring of such processes inside bioreactor culture systems.

1. Introduction

Research during the last decade has demonstrated the huge potential of human embryonic stem cells (hESCs) for biomedical applications, including regenerative medicine [1], drug discovery [2] or heart development and disease modeling [3]. However, the full realization of this potential relies on robust and standardized bioprocessing technologies to ensure optimized and reproducible culture conditions for the stem cells such that sufficient quantity of differentiated cells with suitable quality can be obtained [4,5]. One of the major challenges in stem cell bioprocessing is the lack of online and real-time quantitative information regarding the conditions of the cells within the bioreactors [4,5]. Current analytical techniques for the characterization of embryonic stem cells in-vitro often employ destructive assays rendering on-line monitoring impossible, or are based on crude estimates which provide only limited insight into the molecular processes (e.g. spontaneous beating of embryoid bodies in hESC-derived cardiomyocyte bioprocessing [6]). Due to these limitations, the bioprocesses are not automated and the optimization of differentiation conditions relies on manual procedures, leading to high costs, labor, time and high cell variability [4,5]. The availability of non-invasive analytical techniques which can be used in an automated manner to monitor repeatedly the properties and the condition of the cells within the bioreactor may enable a more efficient and automated optimization of the bioprocesses as well as provide overall quality assessment of the end-point differentiated cells.

A key feature of Raman micro-spectroscopy (RMS) is that important information regarding the molecular characteristics of live cells grown in-vitro can be measured without requiring labeling or other invasive procedures [7], while maintaining the cells in their physiological conditions and growth medium. Time-resolved Raman spectral measurements (up to several hours) were used to detect molecular changes during apoptosis, such as de-localization of cytochrome c [8] and re-organization of phospholipids [9]. However, the in-vitro differentiation of hESCs involves major molecular changes over days or weeks. Such molecular changes include the early signals which establish the commitment towards a specific differentiation pathway as

* Corresponding author. Tel.: +44 1159515172; fax: +44 1159515180.
E-mail address: ioan.notingher@nottingham.ac.uk (I. Notingher).

0304-4165/$ – see front matter
http://dx.doi.org/10.1016/j.bbagen.2013.01.030

well as the significant changes in the cell chemistry which provides the foundation for the structure and function of the somatic cells. The focus of this study is the cardiomyocyte differentiation of embryoid bodies (EBs) formed by aggregated hESCs. This process involves significant changes in the cells, such as formation of myofibrils required to provide the contractile properties of heart [10], the switch from the glycolytic to the more energy efficient oxidative metabolism is characterized by an expansion of the mitochondrial network [11,12] and accumulation of glycogen in the cytoplasm of the cardiomyocytes [13]. Recent studies have also showed that a high glucose concentration in the culture is a prerequisite for in-vitro cardiomyocyte differentiation of hESCs [14].

RMS has been used for label-free investigations of stem cell differentiation, including live individual cells [15,16] and fixed cells in embryoid bodies [17], and for characterization of hESCs cultured in-vitro with the aim of assessing their differentiation status [18–20]. Recently, RMS was used for label-free characterization of individual cardiomyocytes derived from hESCs [21,22] and high accuracy classification models were reported (97% specificity and 96% sensitivity) [21]. The potential of developing label-free cell-sorting techniques for hESCs-derived CMs based on RMS was also explored [23]. In this study we investigate the use of RMS to measure non-invasively the time-dependent molecular changes during the differentiation of EBs towards cardiac phenotype, a bioprocess spanning several days. In situ spatially- and time-resolved Raman measurements were carried out on EBs grown in defined culture medium for inducing differentiation towards cardiac phenotype.

2. Materials and methods

2.1. Materials, general cell culture and immuno-staining

All tissue culture reagents were purchased from Invitrogen (Paisley, UK) and chemicals were obtained from Sigma-Aldrich (Poole, UK) unless otherwise stated. Mouse embryo fibroblasts and hESC cultures were maintained at 37 °C, 5% CO2, in a humidified atmosphere. The medium was changed daily for hESC culture and every 3–4 days during differentiation.

The hESC line HUES7 was cultured in feeder-free conditions in conditioned medium in a Matrigel-coated flask and cultured using trypsin passaging between passages 17–35, as described previously [24]. Differentiation in defined conditions was achieved by forced aggregation of defined numbers of hESCs [25]. Differentiating embryoid bodies were transferred on day 5 to custom-built micro-bioreactors for Raman spectral measurements.

For immunofluorescence and flow cytometry, EBs or dissociated cells were fixed with 4% paraformaldehyde, permeabilized with 0.1% Triton-X100, and then incubated with anti-α-actinin (1:800) and anti-cardiac troponin I (1:250) for 1 h at room temperature. The secondary antibodies were Cy3 and Alexfluor-488 (1:250; Vector Labs), with staining for 1 h at room temperature. For flow cytometry, cells were then washed in PBS two times before analyzing using the Beckman Coulter FC500 flow cytometer with FlowJo software (Treestar, OR). For immunofluorescence, cell nuclei were stained with 40,6-diamidino-2-phenylindole (DAPI, 100 ng/mL) at 1:1000 dilution in PBS for 5 min at room temperature.

2.2. Analysis of beating frequency for individual cardiomyocytes

Beating frequency analysis was carried out using videos recorded under white-light illumination and software developed in MATLAB (The MathWorks, Natick, MA). The beating frequency at each pixel of the EBs was obtained by calculation using the Fourier transform of the time-dependent intensity shift at each individual pixel as described previously [21].

2.3. Raman micro-spectroscopy measurements and data analysis

A custom-built Raman micro-spectrometer optimized for live-cell studies [21] was used to acquire the Raman spectra of the EBs. A long working distance microscope objective (50×NA 0.50, Leica Microsystems) was used to focus the laser on the samples and collect the Raman scattered light. The power of the 785 nm laser was ~170 mW after objective and the diameter of the laser spot was estimated to be ~3 μm. The spectrometer was calibrated before each experiment using 4-acetamidophenol (ASTM E1840). The spectral resolution was ~1.5 cm^{-1} and accuracy was ~0.5 cm^{-1}.

The micro-bioreactors were based on titanium chambers of 3.5 cm diameter and 1.5 cm height, which included a MgF_2 cover slip (0.15 mm thick) at the bottom to enable acquisition of Raman spectra and a top glass window to allow routine observation of the cells on the microscope. The inverted microscope (Olympus IX71) was fitted with an environmental enclosure (Solent, UK) to allow the cells to be maintained in physiological conditions (culture medium, 37 °C temperature, 95% relative humidity and 5% CO_2). During the time-course Raman measurements, the EBs were kept inside the sealed micro-bioreactors within the enclosure on the Raman microscope at all time and the culture medium was not replaced. A total of 8 independent EBs were analyzed during this study, 4 beating and 4 non-beating EBs.

The size of the EBs varied from 300 to 500 μm at day 5 of the differentiation, reaching up to 1 mm at day 9. Raman spectral maps of each individual EB were recorded as raster scans with 10 μm steps (60 by 60 or 100 by 120 grids depending on the size of the EBs) and 1 s acquisition time at each position. Although the step size was larger than the laser spot, this value was considered appropriate given that the beating amplitude of the EBs was ~10 μm.

Outlier spectra (typically less that 1% per spectral map contained cosmic rays, spurious bands or large baseline) were replaced with the average of the spectra measured at the four neighboring points. A Raman background spectrum was calculated as the mean of 3600 spectra (60 by 60 grid) measured in the immediate vicinity of each EB. For principal component analysis, the individual Raman spectra in each raster scans were normalized to zero mean and unity standard deviation.

The PCA model was built using standard functions available in MATLAB and included all individual data points (over 180,000 spectra) acquired from the 8 EBs. Raman maps were built by plotting the scores of the principal component that captured the largest amount of spectral variance in the dataset.

3. Results and discussion

3.1. Differentiation protocol

To produce a model system for Raman spectroscopy time-course analysis, we first established the efficiency of the cardiomyocyte differentiation protocol. The HUES7 hESC line was differentiated using defined culture medium to produce embryoid bodies, as previously described [25]. The time-course appearance of α-actinin and cardiac troponin I, which are required for contractile function in cardiomyocytes, was established by immuno-fluorescence for embryoid bodies between day 5 and 10 of differentiation (Fig. 1). The cardiac markers appeared on day 7, which coincided with spontaneous contractile activity. Flow cytometry and immunofluorescence analysis using the cardiomyocyte markers α-actinin and/or cardiac troponin I were carried out on individual cells dispersed from EBs at day 12 of differentiation (not single EB). This indicated that approximately 85% of the cells present in beating EBs were cardiomyocytes, whereas less than 1% were identified in non-beating EBs (Fig. 2).

Since the environmental enclosure on the Raman microscope allowed cells cultured in the bioreactors to be maintained in optimal

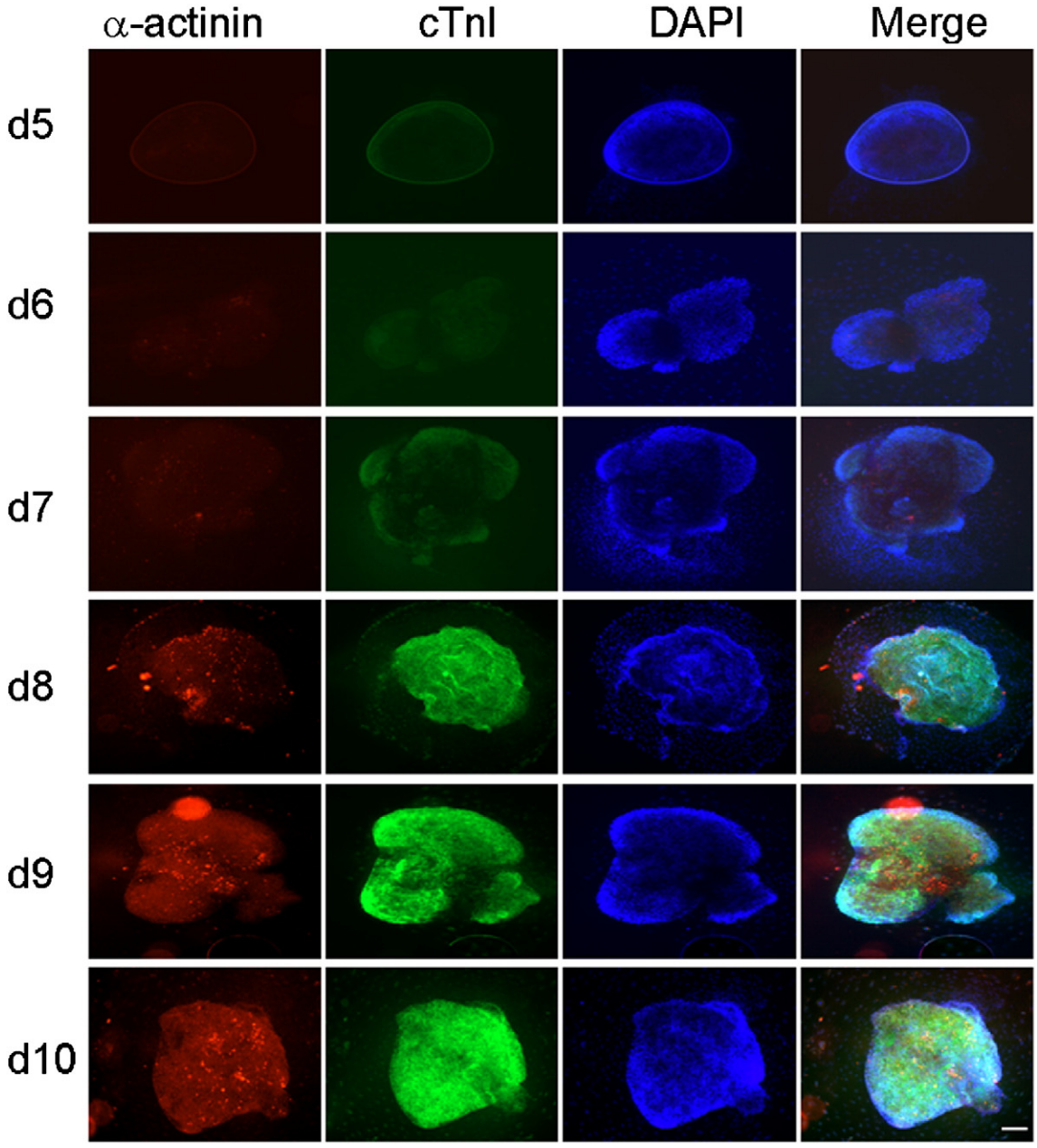

Fig. 1. Cardiac immunostaining of embryoid bodies. From day 5 to 10 of cardiac differentiation (D5–10), embryoid bodies were fixed and stained with the cardiomyocyte markers, α-actinin (red) and cardiac troponin I (cTnI; green). Appearance of the cardiac markers on day 7 corresponded with the onset of spontaneous beating. Samples were counterstained with DAPI to show nuclei. Tricolor images were merged. Scale bar is 200 μm.

conditions for approximately 4–5 days, the time-course Raman spectral measurements of individual EBs were focused on the period between days 5 and 9 of differentiation when, based on the expression of α-actinin and cardiac troponin I (Fig. 1), the appearance of CMs was expected.

3.2. Time-course evolution of the Raman spectra

Fig. 3 shows typical time-course mean Raman spectra (average of all Raman spectra in a raster-scan from which the background was subtracted) for two beating and two non-beating EBs. In agreement with Fig. 1, beating EBs were observed starting with day 7 (videos V1–V4), confirming that the conditions in the micro-bioreactors on the Raman microscope were suitable for achieving cardiac differentiation. The results also confirm that the repeated laser exposure required for the acquisition of time-course Raman spectral maps did not hinder the production of CMs inside EBs during cardiogenic differentiation.

At the early stages of differentiation when no CMs were expected in the EBs (e.g. days 5 and 6), Fig. 3 shows that the mean Raman spectra of all EBs were very similar. The mean Raman spectra described the overall molecular composition of the EBs and their profiles resembled the spectra of hESCs and other cell types reported in the literature [7–23,26].

Raman bands arising from vibrations of proteins can be observed in the 1200–1350 cm^{-1} spectral region (Amide III), 936 cm^{-1} (C–C stretching) and 1450 cm^{-1} (C–H bending). Bands assigned to amino acids can also be identified: phenylalanine (1005 cm^{-1}, 1031 cm^{-1}, 624 cm^{-1}, 1607 cm^{-1}), tyrosine (644 cm^{-1}, 832 cm^{-1}, 854 cm^{-1} and 1607 cm^{-1}) and tryptophan (760 cm^{-1} and 1360 cm^{-1}) [27]. Vibrations of the phosphate groups in nucleic acids produced Raman bands at 788 cm^{-1} (O–P–O stretching) and 1098 cm^{-1}

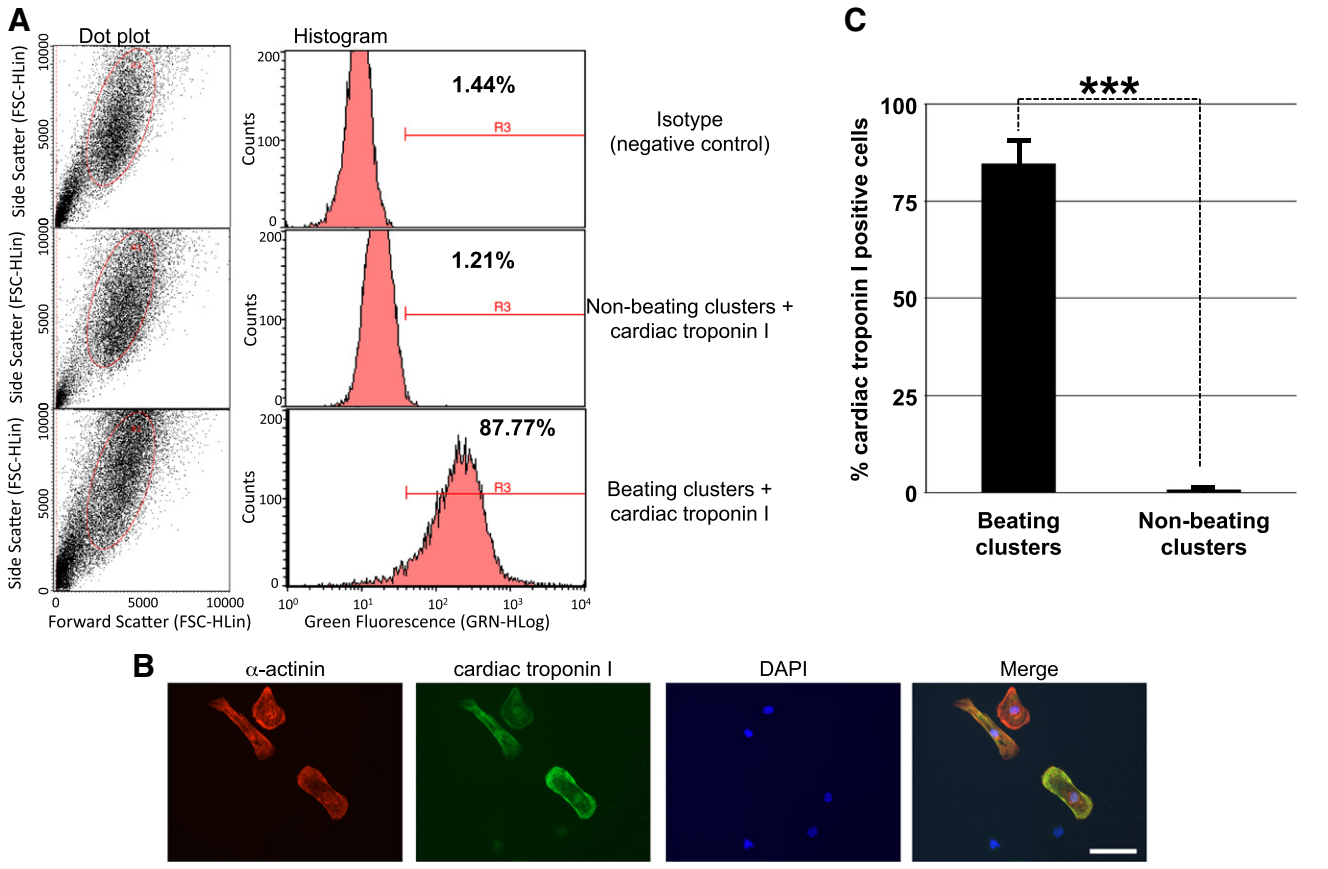

Fig. 2. Cardiomyocyte differentiation efficiency. EBs at day 12 of differentiation were dispersed and incubated with cardiac-specific antibodies. (A) shows a representative example of flow cytometry dot plots and the derived histograms of non-beating or beating EBs stained with a cardiac troponin I antibody, relative to isotype control. (B) shows representative images of a beating EB used for Raman spectral measurements and then dispersed to single cells to quantitate percentage of cardiomyocytes. This example shows that 56% of the cells were double positive for α-actinin and cardiac troponin I. Scale bar = 50 μm. (C) Combined data from flow cytometry and immunofluorescence show 84.6% (±5.4%; SEM, n = 14) of cells in beating EBs stained with α-actinin and/or cardiac troponin I, which is significantly higher ($P<0.001$; *t*-test) than for non-beating EBs (0.85% ± 0.35).

(PO_2-stretching) while bands assigned to the nucleotides can be detected at 729 cm^{-1}, 782 cm^{-1}, 1220–1284 cm^{-1} region, 1342 cm^{-1}, and 1578 cm^{-1} [27]. Spectral bands specifically assigned to the ring bending skeletal modes of carbohydrates can be identified at 482 cm^{-1} and 577 cm^{-1}.

Other molecular vibrations of carbohydrates contribute to the Raman bands at 858 cm^{-1} (CH bending, CH and CH_2 deformation), 937 cm^{-1} (C–O–C glycosidic bond vibration), 1083–1123 cm^{-1} region (C–O and C–C stretching) and 1340 cm^{-1} (C–O–H bending vibration) [27]. Vibrations of the acyl chains in lipids contribute to the bands at 1449 cm^{-1} (CH_2 bending), 1303 cm^{-1} (CH_2 twisting) and 1050–1140 cm^{-1} region (C–C stretching) [27].

Fig. 3 shows significant differences between the Raman spectra of EBs starting with day 7 when the spectra of the beating EBs showed an increase in the intensity of the bands at 482 cm^{-1}, 577 cm^{-1}, 858 cm^{-1}, 937 cm^{-1}, 1083 cm^{-1} and 1340 cm^{-1}. These spectral differences can be more easily observed in the computed difference spectra presented in Fig. 4.

Intense bands at the same frequencies were previously identified in the Raman spectra of isolated beating CMs derived from hESCs and were attributed to the formation of myofibrils and accumulation of glycogen in the CMs [21,23]. These molecular changes are hallmarks for the formation of cardiac tissue and reflect the development of the contractile machinery of the cardiomyocytes [10,13]. A high accumulation of glycogen in hESC-derived CMs was observed by transmission electron microscopy for CMs derived from several hESCs lines [13] and was related to the increase in fuel demand following the switch from the glycolytic metabolism to the oxidative phosphorylation [11,12].

The computed differences between the Raman spectra at different time points (Fig. 4) indicate that additional spectral changes occur during the time evolution of the EBs. Apart from the time-dependent spectral changes taking place preferentially in the beating EBs, Fig. 4 also shows that starting with day 8, a significant increase in a Raman band at 505 cm^{-1} was detected for both beating and non-beating EBs. It is important to notice that the 505 cm^{-1} band was not observed in the Raman spectra of individual cells obtained by dissociation of cell clusters following cardiac differentiation of hESC (CMs and non-CMs) [23]. However, in the referred study, the cells were obtained after dissociation of beating EBs and were grown in fresh culture medium [23]. Thus, the 505 cm^{-1} band may be related to some stress conditions due to the prolonged growth conditions within the bioreactor as the culture medium was not changed to avoid contamination while the standard differentiation protocol requires medium change every 3–4 days. Based on the wavenumber position and the relatively high intensity, this band may be assigned to multiple disulfide bonds that are normally associated with oxidation of two cysteine residues [28].

In the context of hESC differentiation towards the cardiac phenotype, disulphide bonds have been linked to several molecular processes related to protein folding. For example, one quarter of the 100 cysteine residues per subunit of the type 1 ryanodine receptor (RYR1) tetramer are available for covalent modification [29]. The presence of disulfide bonds between the subunits of the RYR1 tetramer was reported to lead to an increase in the release of Ca^{2+} into cytosol with dramatic effects on the beating function of the EBs [30]. Other processes, like cardiac hypertrophy are also influenced by oxidative stress where Thioredoxin 1 (Trx1) catalyzes the reduction of cysteine

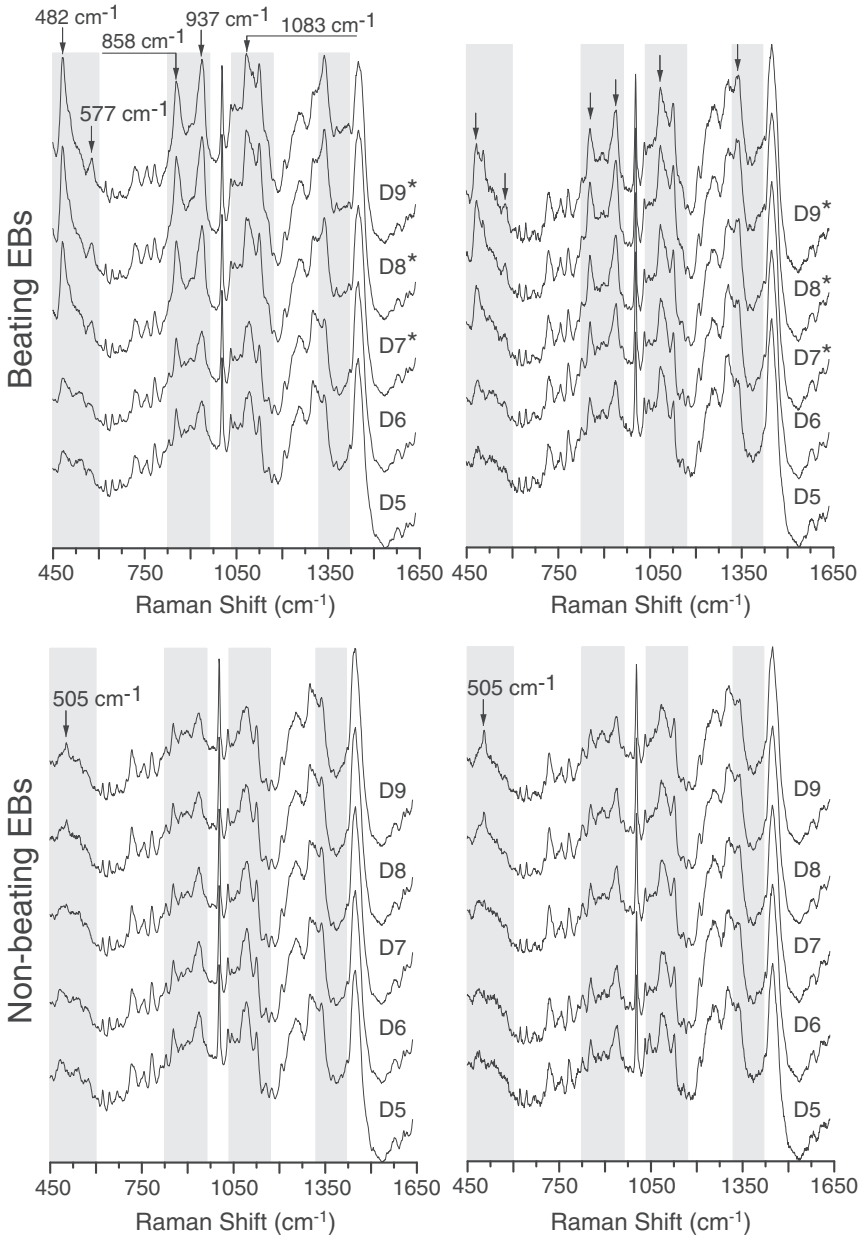

Fig. 3. Time-course mean Raman spectra of two typical beating and two non-beating EBs during day 5–9 (D5–9) of differentiation. The star (*) indicates the days at which beating of the EBs was observed.

disulfides in class II histone deacetylaze (HDAC) proteins [31]. Therefore, the increase in the intensity of the 505 cm^{-1} band at day 8, one day after the expected onset of spontaneous beating of EBs, may be linked to a possible signal of oxidative stress processes that take place during differentiation. Although an accurate assignment of the 505 cm^{-1} Raman band to a specific cellular process requires further investigations, these results demonstrate the ability to obtain molecular information regarding the status of the EBs which may be used as a feedback mechanism to optimize the conditions within the bioreactor.

3.3. Time-course spectral mapping of embryoid bodies

While the average Raman spectra provide information regarding the overall molecular changes of the EBs during differentiation, it is well known that such constructs are highly heterogeneous (also observed in the immuno-fluorescence images for α-actinin in Figs. 1 and 5). For some beating EBs, the CMs were distributed relatively uniformly throughout the EBs, while for other EBs the CMs were grouped in smaller isolated beating clusters of ~500 μm diameter which developed within the same EB. Time-course average Raman spectra from the region indicated by the yellow and green squares for one of the beating EBs in Fig. 5 are presented in the Supplementary Information Fig. S1.

To capture both the temporal and the spatial molecular changes in the EBs during the differentiation, PCA was applied on the time-resolved spectral maps of all EBs. Fig. 5 presents the maps corresponding to the PC1 ("embryoid body PC") scores for the three beating and two non-beating EBs. Retrospective immuno-fluorescence staining for α-actinin is also included in Fig. 5. Considering that this principal component captured ~12.2% of the spectral variance, the results indicate that RMS has a high sensitivity to detect molecular changes related to the cardiomyocyte differentiation. Fig. 5 confirms that at days

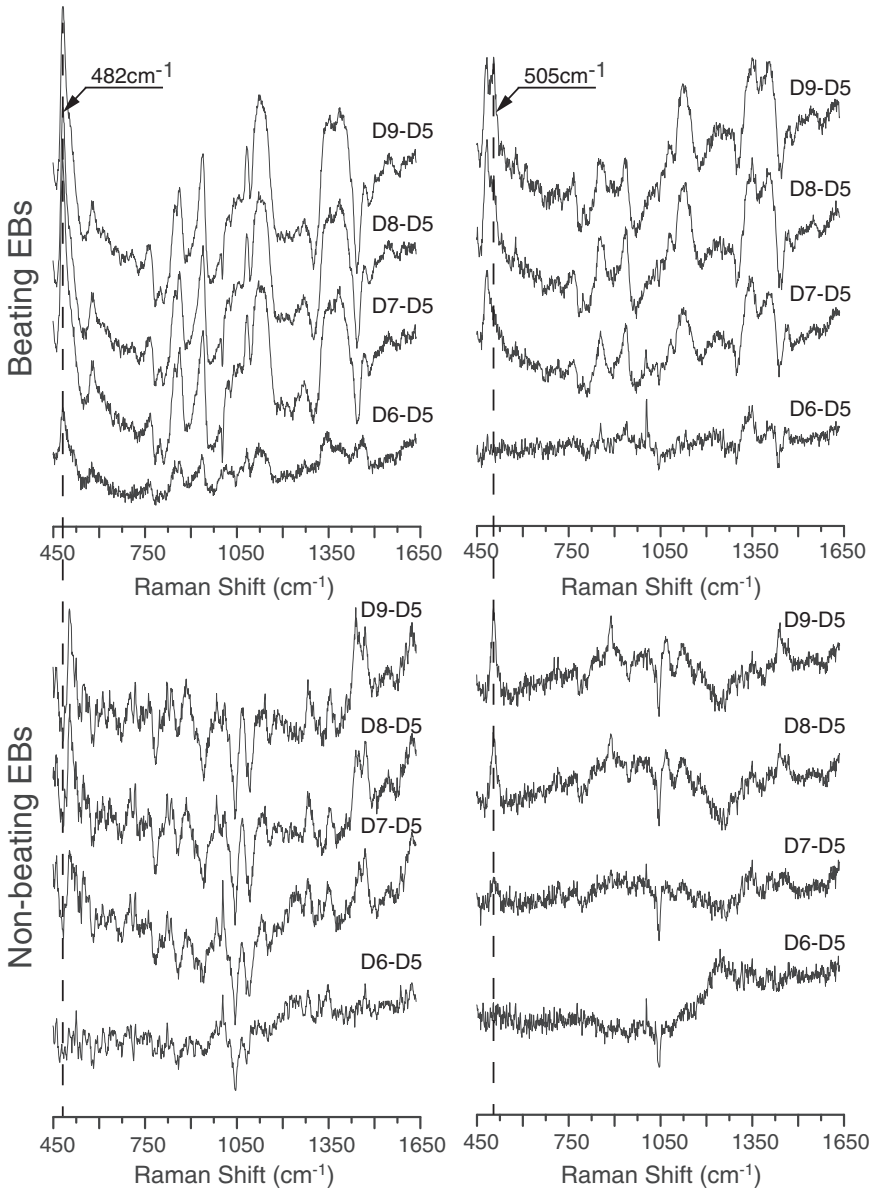

Fig. 4. The time-dependent computed difference spectra D*i*–D5 for two beating and two non-beating EBs. D*i* and D5 represent the mean Raman spectra at day $i = 6$–9 and day 5.

5 and 6, no CMs were observed in the EBs. Starting with day 7, the spectral maps showed the appearance of CMs, either within the entire volume or at the edges, in the beating EBs, while no relative increase in the "embryoid body PC" scores could be detected for the non-beating EBs. Side by side maps representing the beating frequency of the EBs, Raman score maps of "embryoid body PC" together with the immunofluorescence staining for α-actinin are shown in Supplementary Information Fig. S3 for comparison. The frequency maps of the beating EBs highlight the regions of the EBs where the beating was more pronounced and their distribution is in good agreement with the immuno-fluorescence images for α-actinin and with the Raman score maps of the "embryoid body PC".

While the loading spectrum of PC2 indicates mainly variations in the baseline and background signals originating probably from the morphological differences among the EBs, the other principal components consisted of numerous positive and negative peaks within the "spectral fingerprint region", highlighting the complexity of the temporal and spatial molecular changes during the differentiation of hESCs (loading spectra included in Supplementary Information Fig. S2).

3.4. Time-course evaluation of cardiomyocyte-differentiation efficiency of EBs

Recently, label-free spectral discrimination model for identification of individual live hESCs-derived CMs from non-CMs with >95% sensitivity and 97% specificity has been proposed [21]. A "Cardiac PC" was obtained by principal component analysis of Raman spectra obtained from measurements of isolated hESC-derived CMs following dissociation of EBs, and contained strong bands at 858 cm^{-1}, 937 cm^{-1}, 1083 cm^{-1} and 1340 cm^{-1}. A side by side comparison between the "Cardiac PC" and "embryoid body PC" (Fig. 6B) shows that, in addition to these bands, the "embryoid body PC" obtained from the space–time PCA of the Raman spectra of intact EBs investigated in this study contains additional information in the 436–600 cm^{-1} region (strong band at 482 cm^{-1} and 577 cm^{-1}). The computed difference spectrum "Cardiac PC" minus "embryoid body PC" is also included and highlights four major bands at 939 cm^{-1}, 1045 cm^{-1}, 1084 cm^{-1} and 1339 cm^{-1}, which can be attributed to molecular vibrations of carbohydrates. It is interesting to note that

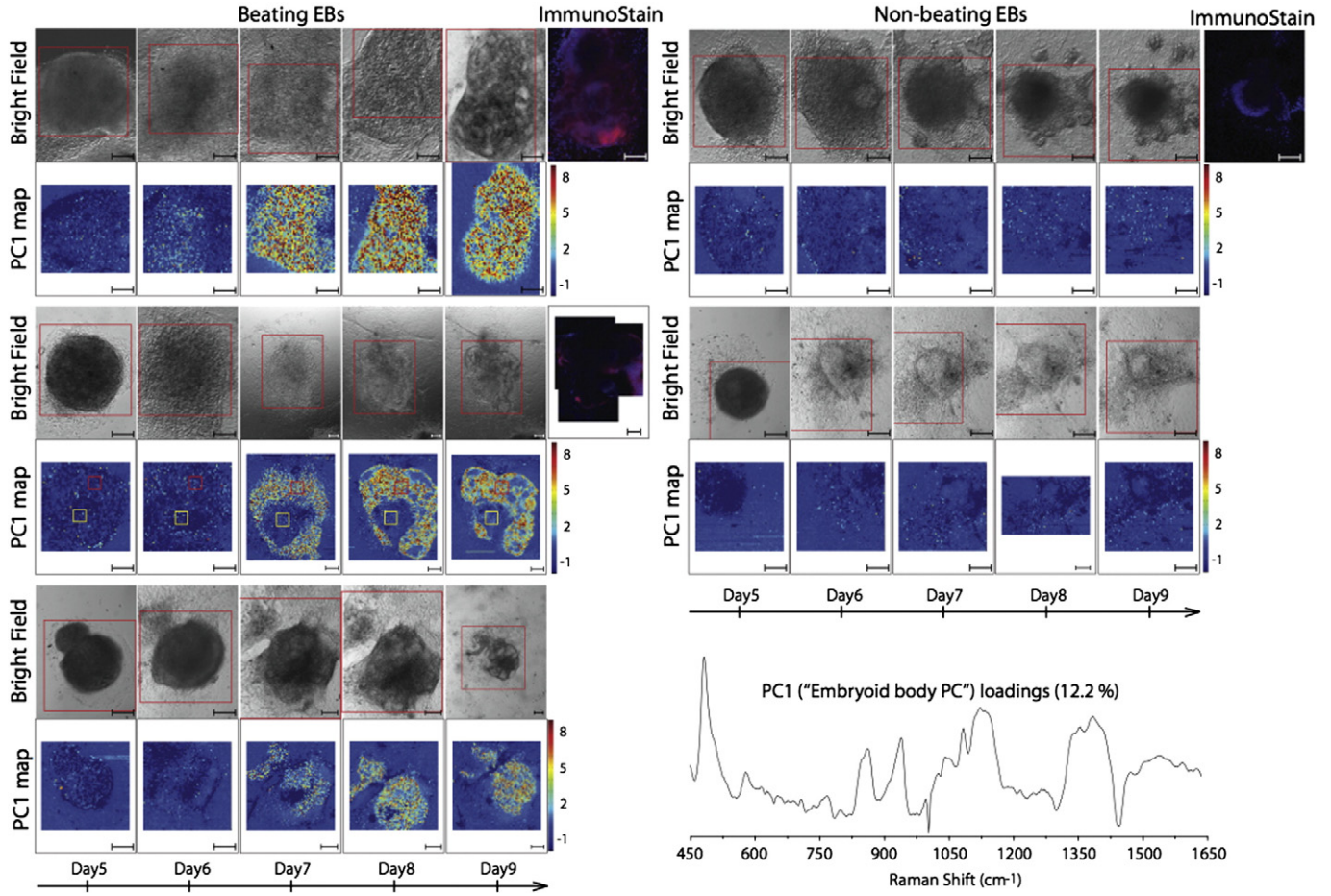

Fig. 5. Principal component analysis of the Raman spectral maps for three beating and two non-beating EBs. Images represent the time-dependent bright field micro-graphs and maps of the "embryoid body PC". Corresponding immuno-fluorescence images for α-actinin (red) and DAPI (blue) are included for comparison. Time-course Raman average spectra corresponding to the regions highlighted by the yellow and red squares are presented in Supplementary Information Fig. S1 (videos available as V1-V4). Scale bars 150 μm.

the 1045 cm^{-1} vibration is significantly stronger in the case of "Cardiac PC" and might be an indication of changes in glycogen metabolism between isolated cells and aggregated cells inside EBs.

To demonstrate the robustness of the RMS in the estimation of the relative abundance of cardiomyocytes, the "Cardiac PC" was used for estimation of the relative CM abundance within the EBs investigated in this study (only the common spectral region 600 cm^{-1} to 1636 cm^{-1} was used in the analysis). Fig. 6A presents the time-dependence of the scores obtained by calculating the projection of the mean Raman spectra on the "Cardiac PC". For the non-beating EBs, the projection scores remained close to zero during the entire measurement period indicating that no CMs were present in the EBs. This finding was confirmed by the immuno-fluorescence images which showed no expression of α-actinin (Fig. 5). However, for the beating EBs the scores increased at day 7, commonly peaked at day 8 and tended to plateau at day 9. The sharp increase at day 7 was consistent with the beating onset. The results also show that the values of the projection scores for the "Cardiac PC" varied considerably among the beating EBs. The α-actinin images at day 9 for the same EBs (after fixation) confirmed the presence of CMs in the beating EBs and also indicated that the EBs with high Raman scores showed higher intensity in the α-actinin staining.

4. Conclusions

This study shows that RMS can be used for in-situ non-invasive monitoring of the cardiac differentiation of embryoid bodies, which may find applications in automated online monitoring of stem cell bioprocesses. EBs cultured in-vitro and induced to differentiate towards the cardiac phenotype were maintained in purpose-designed micro-bioreactors on the Raman microscope for 5 days and spatially-resolved Raman spectra were acquired at 24 h intervals. The successful cardiomyocyte differentiation process was confirmed by beating EBs and high expression of α-actinin indicated that the measurements of the Raman spectra did not affect the viability of the EB or their ability to produce differentiated cardiomyocytes. The time-dependent spectra showed that the beginning of beating at day 7 of differentiation coincided with an increase in the Raman bands previously identified and used as spectral markers for label-free identification of hESC-derived cardiomyocytes. In addition, two more bands in the lower frequency spectral range (482 cm^{-1} and 577 cm^{-1} assigned to the ring bending skeletal modes of carbohydrates) were found to have high intensity in the Raman spectra of cardiomyocyte-rich regions of beating EBs. Considering that these bands are isolated from the other major Raman bands of the cells, they may be used in a single wavelength detection setup, which could make this technique highly attractive for on-line non-invasive continuous monitoring of such processes inside bioreactor culture systems. The spectral maps corresponding to these bands had a high positive correlation with the staining of the EBs for α-actinin at the end of the Raman measurements (day 9). The spectral maps also showed that the increase in intensity of these bands was only found in the regions of beating EBs where a large number of CMs were present. Further developments of this technique and the integration with more advanced bioreactor technologies may allow non-invasive quality assessment of the end-product differentiated cells or enable a more efficient optimization of the bioprocesses.

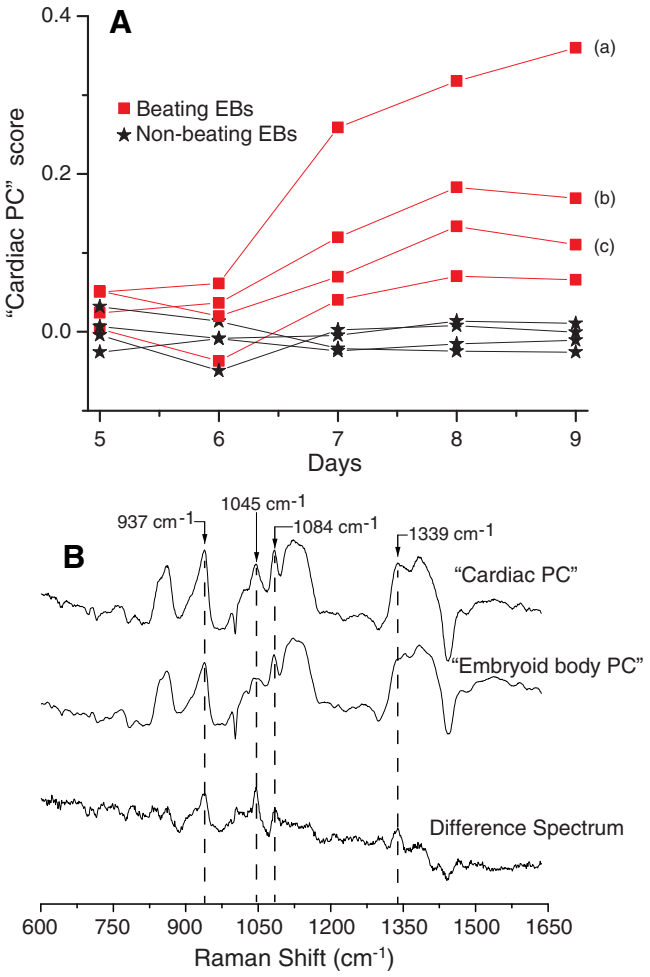

Fig. 6. (A) The time-dependence of the scores obtained by calculating the projection of the mean Raman spectra on the "Cardiac PC" [21] for four beating and four non-beating EBs. (B) Comparison between the "embryoid body PC" and "Cardiac PC" together with the computed difference spectrum. (a), (b) and (c) correspond to the beating EBs from Fig. 5.

Supplementary data to this article can be found online at http://dx.doi.org/10.1016/j.bbagen.2013.01.030.

Acknowledgements

This study was funded by the Biotechnology and Biological Sciences Research Council, UK (BB/G010285/1).

References

[1] L.W. van Laake, R. Passier, P.A. Doevendans, C.L. Mummery, Human embryonic stem cell-derived cardiomyocytes survive and mature in the mouse heart and transiently improve function after myocardial infarction, Stem Cell Res. 1 (2007) 9–24.
[2] S.R. Braam, R. Passier, C.L. Mummery, Cardiomyocytes from human pluripotent stem cells in regenerative medicine and drug discovery, Trends Pharmacol. Sci. 30 (2009) 536–545.
[3] K. Musunuru, I.J. Domian, K.R. Chien, Stem cell models of cardiac development and disease, Annu. Rev. Cell Dev. Biol. 26 (2010) 667–687.
[4] M.R. Placzek, I.-M. Chung, H.M. Macedo, S. Ismail, T.M. Blanco, M. Lim, J.M. Cha, I. Fauzi, Y. Kang, D.C.L. Yeo, C.Yip J. Ma, J.M. Polak, N. Panoskaltsis, A. Mantalaris, Stem cell bioprocessing: fundamentals and principles, J. R. Soc. Interface 6 (2009) 209–232.
[5] E. Ratcliffe, R.J. Thomas, D.J. Williams, Current understanding and challenges in bioprocessing of stem cell-based therapies for regenerative medicine, Br. Med. Bull 100 (2011) 137–155.
[6] H. Yang, Y. Zhang, Z. Liu, P. Chen, K. Ma, C. Zhou, Mouse embryonic stem cell-derived cardiomyocytes express functional adrenoceptors, Biochem. Biophys. Res. Commun. 368 (2008) 887–892.
[7] G.J. Puppels, F.F. de Mul, C. Otto, J. Greve, M. Robert-Nicoud, D.J. Arndt-Jovin, T.M. Jovin, Studying single living cells and chromosomes by confocal Raman microspectroscopy, Nature 347 (1990) 301–303.
[8] M. Okada, N.I. Smith, A.F. Palonpon, H. Endo, S. Kawata, M. Sodeoka, K. Fujita, Label-free Raman observation of cytochrome c dynamics during apoptosis, Proc. Natl. Acad. Sci. U.S.A. 109 (2012) 28–32.
[9] A. Zoladek, F.C. Pascut, P. Patel, I. Notingher, Non-invasive time-course imaging of apoptotic cells by confocal Raman micro-spectroscopy, J. Raman Spectrosc. 42 (2011) 251–258.
[10] M. Snir, I. Kehat, A. Gepstein, R. Coleman, J. Itskovitz-Eldor, E. Livne, L. Gepstein, Assessment of the ultrastructural and proliferative properties of human embryonic stem cell-derived cardiomyocytes, Am. J. Physiol. Heart Circ. Physiol. 285 (2003) H2355–H2363.
[11] J.C. St John, J. Ramalho-Santos, H.L. Gray, P. Petrosko, V.Y. Rawe, C.S. Navara, C.R. Simerly, G.P. Schatten, The expression of mitochondrial DNA transcription factors during early cardiomyocyte in vitro differentiation from human embryonic stem cells, Cloning Stem Cells 7 (2005) 141–153.
[12] S. Chung, P.P. Dzeja, R.S. Faustino, C. Perez-Terzic, A. Behfar, A. Terzic, Mitochondrial oxidative metabolism is required for the cardiac differentiation of stem cells, Nat. Clin. Pract. Cardiovasc. Med. 4 (2007) S60–S67.
[13] M. Gherghiceanu, L. Barad, A. Novak, I. Reiter, J. Itskovitz-Eldor, O. Binah, L.M. Popescu, Cardiomyocytes derived from human embryonic and induced pluripotent stem cells: comparative ultrastructure, J. Cell. Mol. Med. 15 (2011) 2539–2551.
[14] F.L. Crespo, V.R. Sobrado, L. Gomez, A.M. Cervera, K.J. McCreath, Mitochondrial reactive oxygen species mediate cardiomyocyte formation from embryonic stem cells in high glucose, Stem Cells 28 (2010) 1132–1142.
[15] I. Notingher, I. Bisson, A.E. Bishop, W.L. Randle, J.M. Polak, L.L. Hench, In situ spectral monitoring of mRNA translation in embryonic stem cells during differentiation in vitro, Anal. Chem. 76 (2004) 3185–3193.
[16] A. Ghita, F.C. Pascut, M. Mather, V. Sottile, I. Notingher, Cytoplasmic RNA in undifferentiated neural stem cells: a potential label-free Raman spectral marker for assessing the undifferentiated status, Anal. Chem. 84 (2012) 3155–3162.
[17] E. Zuser, T. Chernenko, J. Newmark, M. Miljković, M. Diem, Confocal Raman microspectral imaging (CRMI) of murine stem cell colonies, Analyst 135 (2010) 3030–3033.
[18] H.G. Schulze, S.O. Konorov, N.J. Caron, J.M. Piret, M.W. Blades, R.F. Turner, Assessing differentiation status of human embryonic stem cells noninvasively using Raman microspectroscopy, Anal. Chem. 82 (2010) 5020–5027.
[19] S.O. Konorov, H.G. Schulze, J.M. Piret, S.A. Aparicio, R.F. Turner, M.W. Blades, Raman microscopy-based cytochemical investigations of potential niche-forming inhomogeneities present in human embryonic stem cell colonies, Appl. Spectrosc. 65 (2011) 1009–1016.
[20] S.O. Konorov, H.G. Schulze, C.G. Atkins, J.M. Piret, S.A. Aparicio, R.F. Turner, M.W. Blades, Absolute quantification of intracellular glycogen content in human embryonic stem cells with Raman microspectroscopy, Anal. Chem. 83 (2011) 6254–6258.
[21] F.C. Pascut, H.T. Goh, N. Welch, L. Buttery, C. Denning, I. Notingher, Non-invasive detection and imaging of molecular markers in live cardiomyocytes derived from human embryonic stem-cells, Biophys. J. 100 (2011) 251–259.
[22] J.W. Chan, D.K. Lieu, T. Huser, A.L. Li, Label-free separation of human embryonic stem cells and their cardiac derivatives using Raman spectroscopy, Anal. Chem. 81 (2009) 1324–1331.
[23] F.C. Pascut, H.T. Goh, V. George, C. Denning, I. Notingher, Toward label-free Raman-activated cell sorting of cardiomyocytes derived from human embryonic stem cells, J. Biomed. Opt. 16 (2011) 045002.
[24] P.W. Burridge, D. Anderson, H. Priddle, M.D. Barbadillo Muñoz, S. Chamberlain, C. Allegrucci, L.E. Young, C. Denning, Improved human embryonic stem cell embryoid body homogeneity and cardiomyocyte differentiation from a novel V-96 plate aggregation system highlights interline variability, Stem Cells 25 (2007) 929–938.
[25] P.W. Burridge, S. Thompson, M.A. Millrod, S. Weinberg, X. Yuan, A. Peters, V. Mahairaki, V.E. Koliatsos, L. Tung, E.T. Zambidis, A universal system for highly efficient cardiac differentiation of human induced pluripotent stem cells that eliminates interline variability, PLoS One 6 (2011) e18293.
[26] I. Notingher, L.L. Hench, Raman microspectroscopy: a noninvasive tool for studies of individual living cells in vitro, Expert Rev. Med. Devices 3 (2006) 215–234.
[27] A.T. Tu, Raman Spectroscopy in Biology: Principles and Applications, John Wiley and Sons, New York, 1982.
[28] E.J. Bastian Jr., R.M. Martin, Disulfide vibrational spectra in the sulfur–sulfur and carbon–sulfur stretching region, J. Phys. Chem. 77 (1973) 1129–1133.
[29] A. Dulhunty, C. Haarmann, D. Green, J. Hart, How many cysteine residues regulate ryanodine receptor channel activity? Antioxid. Redox Signal. 2 (2000) 27–34.
[30] B. Aghdasi, J.-Z. Zhang, Y. Wu, M.B. Reid, S.L. Hamilton, Multiple classes of sulfhydryls modulate the skeletal muscle Ca2+ release channel, J. Biol. Chem. 272 (1997) 3739–3748.
[31] S. Oka, T. Ago, T. Kitazono, D. Zablocki, J. Sadoshima, The role of redox modulation of class II histone deacetylases in mediating pathological cardiac hypertrophy, J. Mol. Med. 87 (2009) 785–791.